Control and Analysis of Droop and Reverse Droop Controllers for Distributed Generations

Wu, Dan; Tang, Fen; Vasquez, Juan Carlos; Guerrero, Josep M.

Published in:
Proceedings of the 11th International Multiconference on Systems, Signals & Devices, SDD 2014

DOI (link to publication from Publisher):
10.1109/SSD.2014.6808842

Publication date:
2014

Document Version
Early version, also known as pre-print

Control and Analysis of Droop and Reverse Droop Controllers for Distributed Generations

Dan Wu[1], Fen Tang[1,2], Juan C. Vasquez[1], and Josep M. Guerrero[1]
[1] Department of Energy Technology, Aalborg University. Denmark
{dwu , juq , joz}@et.aau.dk
[2] School of Electrical Engineering, Beijing Jiaotong University, P. R. China
ftang_nego@126.com

***Abstract*—This paper addresses control and analysis of droop and reverse droop control for distributed generations (DG). The droop control is well known applied to the voltage control mode (VCM) DG units, but has limitation when implemented on the current control mode (CCM) units. Therefore, this paper gives a more complete primary control for DG systems that integrates with both VCM and CCM units. The power management can be uniformly achieved by designing proportional droop and reverse droop parameters. And the power sharing effect among CCM and VCM DG units is discussed. Finally, hardware-in-the-loop simulations are carried out to validate the proposed control and analysis.**

***Index Terms*—Distributed generation, droop control, reverse droop control.**

I. INTRODUCTION

With the fast development of power electronic technologies, distributed generation (DG) is emerging as a promising form of power supply compared to the traditional centralized power distribution. To meet the demand of power consumption of loads, the control of DG units has drawn great attention in recent years. According to different control objectives, DG units can be classified into grid forming units and grid following units [1]. The grid forming units are usually controlled in voltage control mode (VCM) to generate the grid frequency and voltage, so that to "form" grid. While the grid following units are controlled in current control mode (CCM) to generate active and reactive power based on the synchronized phase from grid. The control modes of VCM and CCM are decided by the control structure of innerloop of each DG unit, and many literatures has addressed in order to improve the innerloop performance with VCM and CCM units [2-4].

However, with only innerloop control the system is hard to get capability to manage power among DG units since the converters have no inertia compare to conventional synchronous generators. In this sense, droop control is proposed to achieve wireless power management among DG units [5,6]. In the previous literatures, many researches have been carried out to improve the performance of droop control. For example, phase shift control is proposed in order to improve the dynamic performance [7], virtual impedance can be applied with droop control to decouple the active/reactive power regulation [8]. These droop control strategies are very effective when applied to the DG units in VCM. While for the DG units in CCM that applied in most renewable sources, the droop control cannot be implemented directly since the output of droop control is voltage amplitude and frequency. And few researches have been found to analyze the primary control of DG units in CCM. Therefore, the control and analysis of droop and reverse droop control for both VCM and CCM DG units are carried out in this paper. Active and reactive power can be wireless managed in a DG system consists of both VCM and CCM units. And the CCM units are also able to participate in the bus voltage and frequency regulation. The paper is organized as follows, Section II gives the fundamentals of droop and reverse droop control. Section III shows the control implementation of VCM and CCM DG units. Section IV shows the hardware-in-the-loop simulation results based on a three DG units system to verify the proposed control.

II. FUNDAMENTALS OF DROOP/ REVERSE DROOP METHOD

Fig. 1 shows the equivalent circuit of a DG converter connected to AC bus through output impedance, where E and V are the amplitude of the converter output voltage and AC bus voltage respectively, ϕ is the power angle between the converter and the AC bus, $Z\angle\theta$ is the output impedance of DG. Usually the output impedance is considered highly inductive, and then the output active and reactive power can be considered as proportional to the power angle and output voltage amplitude [5],

$$P \propto \phi \tag{1}$$

$$Q \propto E \tag{2}$$

In terms of controlling the output power of DG units, the control algorithms can be classified as VCM and CCM. For VCM converters, the active and reactive power are regulated with droop control in the primary level, which is described as

$$\omega = \omega^* - m_d P \tag{3}$$

$$E = E^* - n_d Q \tag{4}$$

where ω is the nominal output frequency of converters, m_d and n_d are the droop coefficients. The power regulation characteristic with droop control is shown in Fig. 2. For the parallel connected VCM converters, the power distribution and management are achieved by assigning proper droop coefficient of each converter, which is shown as

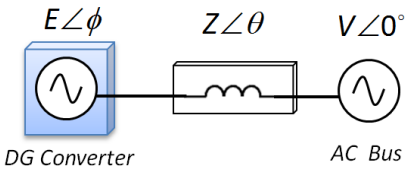

Fig. 1. Equivalent circuit of a DG converter connected to AC MG bus.

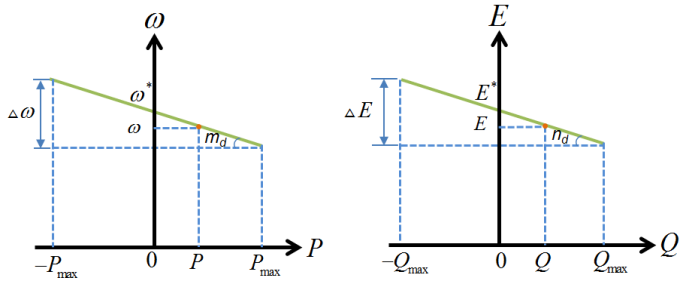

Fig. 2. Power regulation characteristic with droop control.

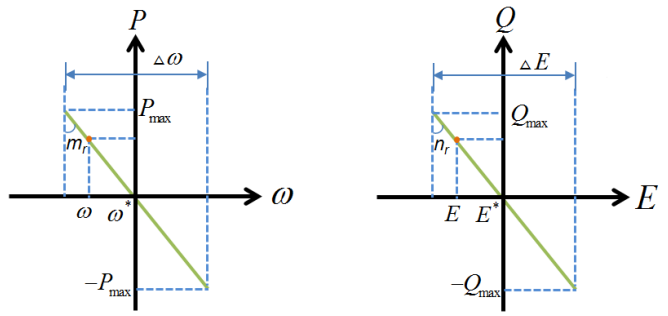

Fig. 3. Power regulation characteristic with reverse droop control.

$$P_1 : P_2 \cdots : P_i = \frac{1}{m_1} : \frac{1}{m_2} \cdots : \frac{1}{m_i} \tag{5}$$

$$Q_1 : Q_2 \cdots : Q_i = \frac{1}{n_1} : \frac{1}{n_2} \cdots : \frac{1}{n_i} \tag{6}$$

For the CCM converters, the active and reactive power is regulated directly by inner current loop. In order to contribute to regulate the AC bus frequency and amplitude, reverse droop can be applied as,

$$P^* = \frac{1}{m_r}(\omega^* - \omega_g) \tag{7}$$

$$Q^* = \frac{1}{n_r}(E^* - E_g) \tag{8}$$

where ω_g and E_g are the measured frequency and amplitude of bus voltage, m_r and n_r are the reverse droop parameters. Fig. 3 shows the power regulation characteristic with reverse droop control. Compare (7) and (8) with (3) and (4), suppose ideal measurement with frequency and amplitude of bus voltage (i.e. $\omega_g = \omega$, $E_g = E$), and $m_d = m_r$, $n_d = n_r$, then equal power sharing can be obtained between VCM and CCM DG units. In fact, by assigning proportional droop and reverse droop coefficients in primary level, the proper power distribution can be obtained

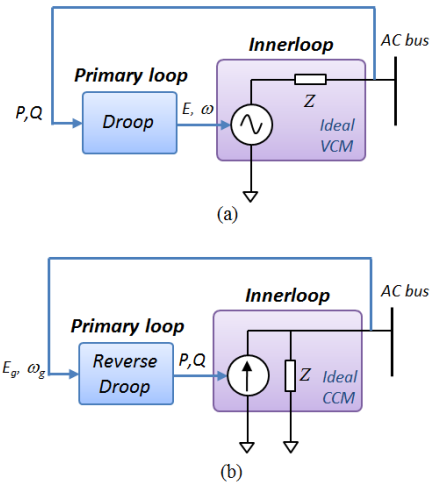

Fig. 4. Simplified system configuration of VCM and CCM.

not only in parallel VCM systems and CCM systems respectively but also in integrated VCM and CCM DG systems, which is consistent expressed in (5) and (6).

The simplified system configuration of VCM and CCM with droop and reverse droop is shown in Fig. 4. With only innerloop of VCM, the system operates as an ideal grid forming unit to fix constant bus voltage and frequency; with only innerloop of CCM, the system operates as an ideal grid following unit to deliver constant power. The additional primary loops based on droop and reverse droop control make the systems have capability to regulate active/reactive power and bus voltage/frequency.

III. Control Implementation of Droop/ Reverse Droop Method

The control algorithms for the three-phase VCM/CCM converters are shown in Fig. 5 and Fig. 6, which are classified into innerloop control and droop/reverse droop control.

A. Innerloop Control of VCM and CCM

The innerloop control of VCM aims at obtaining good output voltages regulation with respect to determined capacitor voltage reference. Firstly, the three-phase *abc* variables are transformed into two-phase *dq* variables with reference frame transformation $T_{abc/dq0}$. Then PI controllers are implemented into voltage and current loops to eliminate steady state errors similar with direct current control systems. At last, the output *dq* control variables are transformed back into *abc* variables with inverse transformation $T^{-1}_{dq0/abc}$.

While for the innerloop control of CCM, the objective is to obtain good output power regulation. Therefore, the innerloop compromises a single PI current controller in *dq* reference frame, with reference frame transformation $T_{abc/dq0}$ and $T^{-1}_{dq0/abc}$.

B. VCM Primary Droop control

As shown in Fig. 5, the primary droop control of VCM includes power calculation block, droop method and voltage reference generator. The instant power theory is applied in the power calculation block, which is shown as

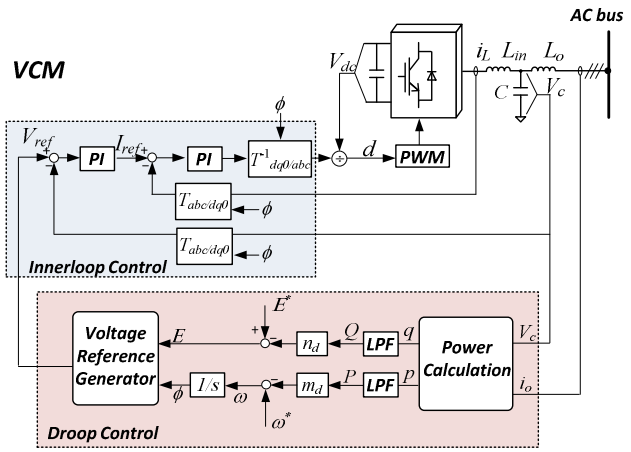

Fig. 5. Control Algorithm of VCM.

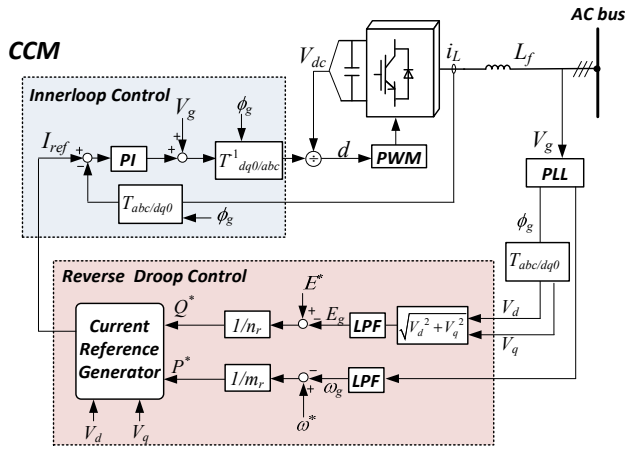

Fig. 6. Control Algorithm of CCM.

$$p = v_{cd} i_{od} + v_{cq} i_{oq} \tag{9}$$

$$q = v_{cq} i_{od} - v_{cd} i_{oq} \tag{10}$$

Where p and q are the instant power flow to AC bus, v_{gd} and v_{gq} are the grid voltages in dq reference frame, i_{od} and i_{oq} are the output currents in dq reference frame. Then based on (3) and (4), the output frequency and amplitude is generated for power regulation control. The droop coefficient should be designed with limitation of power ratings [8],

$$m_d = \frac{\Delta\omega}{P_{\max V}} \tag{11}$$

$$n_d = \frac{\Delta E}{Q_{\max V}} \tag{12}$$

where $\Delta\omega$ and ΔE are the maximum allowable bus frequency and voltage deviation, $P_{\max V}$ and $Q_{\max V}$ are the maximum active power and reactive power of each unit. The LPF block represents a low-pass filter for the power calculation which determines the primary loop bandwidth. Finally, the output voltage command which is sent to the innerloop voltage control is generated as $V_{dref} = E$ and $V_{qref} = 0$.

C. CCM Primary Reverse Droop Control

As shown in Fig. 6, the primary reverse droop control of CCM includes grid voltage and frequency estimation, reverse droop method and current reference generator. First of all, a simple phase lock loop (PLL) [9] is used for the estimation of grid voltage amplitude and frequency. Then with reverse droop of (7) and (8), the power reference P^* and Q^* is obtained. The reverse droop coefficient is designed within the limitation of

$$m_r = \frac{\Delta\omega}{P_{\max C}} \tag{13}$$

$$n_r = \frac{\Delta E}{Q_{\max C}} \tag{14}$$

Where $P_{\max C}$ and $Q_{\max C}$ are the available active power and reactive power of CCM unit. It should also be noted that depending on the power line impedance value among converters, reactive power may not be accurately shared among units as the active power. In fact, this reactive power difference can be calculated as

$$Q_{div} = \frac{E_{div}}{n_r} \tag{15}$$

where Q_{div} and E_{div} are the reactive power of converters and voltage amplitude difference over output impedance between two DG units. It can be seen that depending on various reverse droop coefficients, there is a tradeoff between the reactive power sharing accuracy and output voltage regulation, which is consistent with droop control converters. Finally, the current references is generated as

$$i_{dref} = \frac{v_{gd} \cdot P^* + v_{gq} \cdot Q^*}{\sqrt{v_{gd}^{\ 2} + v_{gq}^{\ 2}}} \tag{16}$$

$$i_{qref} = \frac{v_{gq} \cdot P^* - v_{gd} \cdot Q^*}{\sqrt{v_{gd}^{\ 2} + v_{gq}^{\ 2}}} \tag{17}$$

where i_{dref} and i_{qref} are the generated output currents references, v_{gd} and v_{gq} are the grid side voltage. P^* and Q^* are the active and reactive power regulated from reverse droop control.

IV. Hardware-in-the-Loop Results

In order to validate the droop and reverse droop control strategy for both ESS and RES units, hardware-in-the-loop simulations are carried out based on dspace1006 platform. The system configuration is shown in Fig. 7, the simulated system consists of three DG units, in which the DG_1 operates in VCM with droop control, and DG_2 and DG_3 operate in CCM with reverse droop. The power stage and control system parameters are shown in Table I. In order to evaluate the active power and reactive power sharing performance, the reverse droop confidents are selected the same value considering equal power ratings of converters.

Fig. 8 shows the simulation results of active power sharing among DG units and corresponding output frequency. At t_1 and t_2, DG_2 and DG_3 start respectively. Before t_1, the active power

TABLE I. POWER STAGE AND CONTROLLER PARAMETERS

Parameter	Symbol	Value	Unit
Power Stage			
Nominal Bus Voltage	V^*	230	V
Nominal Bus Frequency	f^*	50	Hz
Filter Inductance of DG_1	L	1.8	mH
Filter Inductance of DG_2 and DG_3	L_f	3.6	mH
Filter Capacitance	C	2200	μF
Output Inductance	L_o	0.1	mH
Load	R,L	43/0.421	Ω/H
Innerloop Control			
Voltage Loop PI	k_{pV}, k_{iV}	0.1, 200	-, s^{-1}
Current Loop PI	k_{pI}, k_{iI}	15,50	-, s^{-1}
Primary Control			
Frequency Droop	m_d	0.003	rad·s^{-1}/W
Voltage Droop	n_d	0.008	V/Var
Frequency Reverse Droop	m_r	0.003	rad·s^{-1}/W
Voltage Reverse Droop	n_r	0.008	V/Var

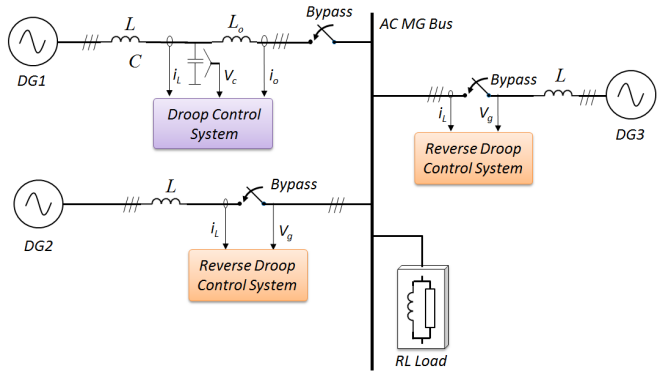

Fig. 7. Control Algorithm of CCM.

of load is supported only by DG_1 with VCM at 1.58kW. At t_1, the DG_2 starts, and the VCM and CCM unit are able to share the active loads at 800W. At t_2, the second CCM unit DG_3 starts, and all DG units share the total active load evenly. It can be seen that the active power can be shared well due to the all the units have common output frequency at AC bus.

Fig. 9 shows the simulation results of reactive power sharing among DG units when n_d=n_r=0.0008 and corresponding output voltage amplitude. The power factor of load is 0.8. Before t_1, the reactive power of load is supported only by DG_1 with VCM at 1.2kVar. The DG_2 starts at t_1, and compared with the conventional reactive power control of CCM that Q^*=0, DG_2 is able to supply reactive power to the loads. However, due to the output voltage difference between DG_1 and DG_2, there is reactive power unbalance in steady state. At t_2, the second CCM unit DG_3 starts, and all DG units supply the reactive power of load commonly. Since CCM units sense common AC bus voltage with PLL, the reactive power can be shared between DG_2 and DG_3, but reactive power unbalance exists between VCM unit and CCM units. Fig. 10 shows the simulation results of reactive power sharing among DG units

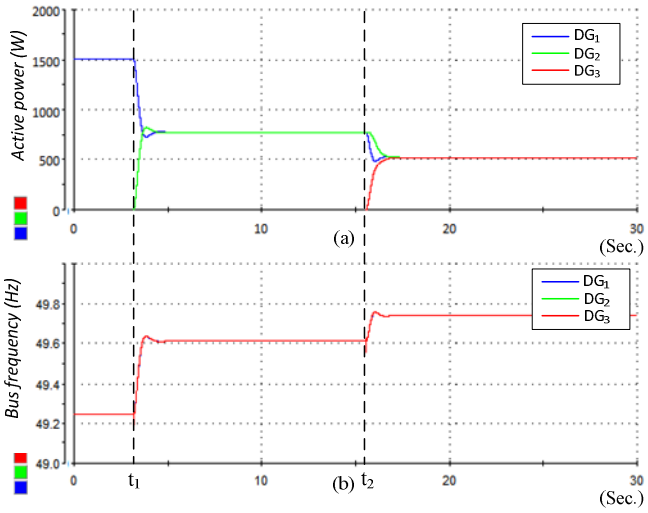

Fig. 8. Active power sharing among DG units (a) and corresponding output frequency (b).

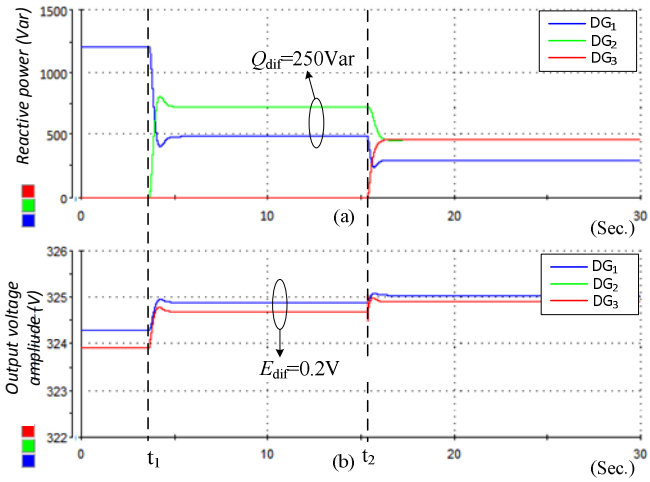

Fig. 9. Reactive power sharing among DG units with n_d=n_r=0.0008 (a) and corresponding output voltage amplitude (b).

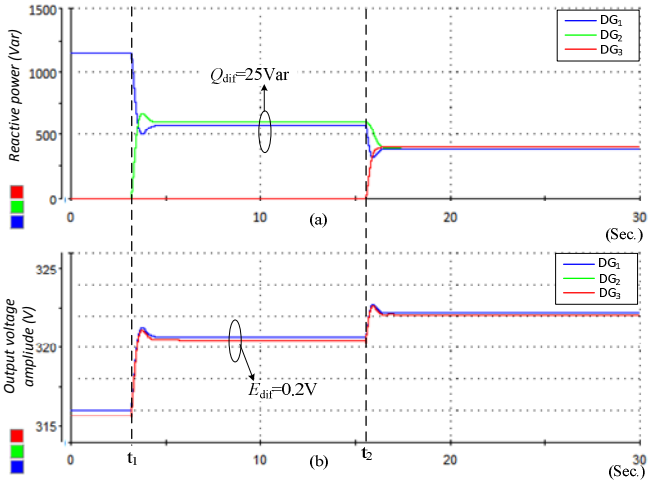

Fig. 10. Reactive power sharing among DG units with n_d=n_r=0.008 (a) and corresponding output voltage amplitude (b).

when n_d=n_r=0.008 and corresponding output voltage amplitude. It can be seen that with the increase of droop and reverse droop coefficients, the reactive power sharing performance can be improved as shown in (15). However, there is a tradeoff between the reactive power sharing accuracy and output voltage deviation.

Fig. 11 and Fig. 12 show that output currents (phase A) of DG_1, DG_2 and DG_3 in steady state with n_d=n_r=0.0008 and 0.008 respectively. It can be observed that there is no circulating currents flow between DG_2 and DG_3, and the circulating currents of VCM (DG_1) and CCM units (DG_2 and DG_3) can be suppressed effectively when increasing droop and reverse droop parameters.

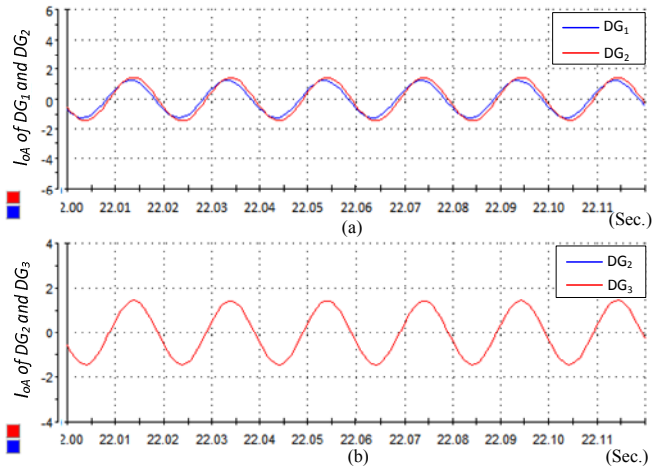

Fig. 11. Steady state output currents of DG_1 and DG_2 (a), and DG_2 and DG_3 (b) with n_d=n_r=0.0008.

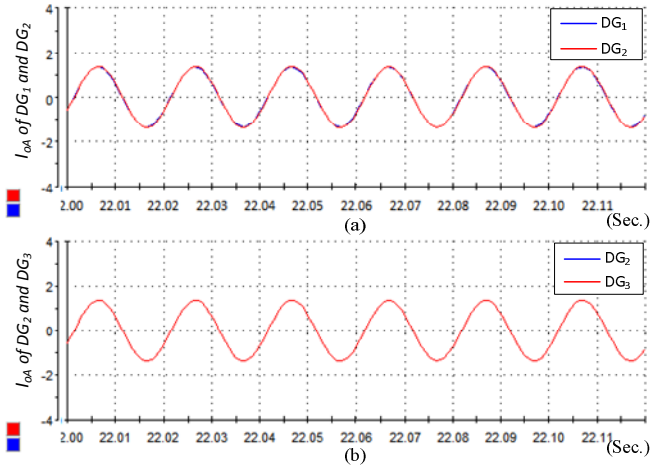

Fig. 12. Steady state output currents of DG_1 and DG_2 (a), and DG_2 and DG_3 (b) with n_d=n_r=0.008.

V. Conclusion

The paper analyzed the droop and reverse droop control that applied with VCM and CCM DG units respectively. With reverse droop control, the CCM units were able to participate in the bus voltage and frequency regulation. Active and reactive power can be uniformly managed with designing droop and reverse droop control parameters proportionally with different modes of DG units within the capability of converters. The power sharing effect by selection of reverse droop parameters is analyzed. At last, simulation results show the validation of the analysis.

References

[1] K. Sun; L. Zhang; Y. Xing; J.M. Guerrero, , "A Distributed Control Strategy Based on DC Bus Signaling for Modular Photovoltaic Generation Systems With Battery Energy Storage," *IEEE Trans. Power Electron.,* vol.26, no.10, pp.3032,3045,

[2] J.M. Guerrero,; L. Hang; J. Uceda, "Control of Distributed Uninterruptible Power Supply Systems," *IEEE Trans. Ind. Electron.*, vol.55, no.8, pp.2845-2859, Aug. 2008.

[3] Zmood, D.N.; Holmes, D.G.; Bode, G.H.; , "Frequency-domain analysis of three-phase linear current regulators ," Industry Applications, IEEE Transactions on , vol.37, no.2, pp.601-610.

[4] J. F. Chen and C.-L. Chu, "Combination voltage-controlled and current controlled PWM inverters for UPS parallel operation," *IEEE Trans. Power Electron.,* vol. 10, no. 5, pp. 547–558, Sep. 1995.

[5] J. M. Guerrero, L. GarciadeVicuna, J. Matas, M. Castilla, and J. Miret, "A Wireless Controller to Enhance Dynamic Performance of Parallel Inverters in Distributed Generation Systems," *IEEE Trans. Power Electron.,* vol. 19, no. 5, pp. 1205–1213, Sep. 2004.

[6] J. C. Vasquez, R. A. Mastromauro, J. M. Guerrero, and M. Liserre, "Voltage Support Provided by a Droop-Controlled Multifunctional Inverter," IEEE Trans. Ind. Electron., vol. 56, no. 11, pp. 4510–4519, Nov. 2009.

[7] Avelar, H.J.; Parreira, W.A.; Vieira, J.B.; de Freitas, L.C.G.; Alves Coelho, E.A., "A State Equation Model of a Single-Phase Grid-Connected Inverter Using a Droop Control Scheme With Extra Phase Shift Control Action," *IEEE Trans. Ind. Electron.*, vol.59, no.3, pp.1527,1537, March 2012

[8] J. M. Guerrero, L. GarciadeVicuna, J. Matas, M. Castilla, and J. Miret, "Output Impedance Design of Parallel-Connected UPS Inverters With Wireless Load-Sharing Control," *IEEE Trans. Ind. Electron.*, vol. 52, no. 4, pp. 1126–1135, Aug. 2005.

[9] S. Chung, "A phase tracking system for three phase utility interface inverters," *IEEE Trans. Power Electron.,* vol.15, no.3, pp.431,438, May 2000